

Automatic Phase Alignment for High Bandwidth Cartesian Feedback Power Amplifiers

Joel L. Dawson and Thomas H. Lee

Center for Integrated Systems

Stanford University

Stanford, CA 94305

Phone: (650)725-4486 Fax: (650)725-3383 Email: jldawson@smirc.stanford.edu

Abstract— We demonstrate a truly continuous regulator of oscillator phase alignment suitable for high bandwidth Cartesian feedback power amplifiers. A new approach to the problem is introduced, which yields a simple nonlinear dynamical controller. Our prototype achieves accurate regulation (3.8 degrees) at the highest baseband bandwidth reported.

I. INTRODUCTION

Presently there exists a great demand for wireless systems that achieve high data transmission rates while using as little power and bandwidth as possible. Maximum data transfer for a given channel width demands sophisticated modulation techniques, the best of which require a linear power amplifier (PA). The strong tradeoff between linearity and power efficiency in PA's has motivated research into linearization techniques, of which Cartesian feedback is an important and promising example [1], [2]. Figure 1 shows a typical Cartesian feedback system.

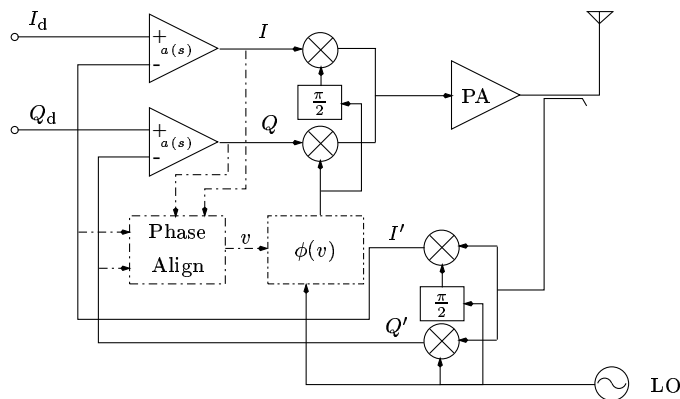


Fig. 1. Typical Cartesian feedback system (this work shown in dashed lines).

The phase shifter in figure 1 is necessary to ensure synchronous demodulation of the baseband signal. Properly adjusted, the system functions as two decoupled feedback loops. Feedback stability margins degrade as this adjustment departs from the optimum, and instability can result. The exact phase shift required can drift over time, temperature, and process variations, and usually changes with carrier frequency, which is particularly troublesome for frequency-hopping systems. To allow for linearization at the maximum symbol rate, this phase shift must be regulated as accurately as possible. In addition, rejection of drift with temperature demands continuous regulation. Ohishi et al. [2] demonstrate a close approximation to this: they exploit the repeated appearance of a predetermined

calibration symbol. Our prototype is the first truly continuous regulator of local oscillator phase alignment, and it completely avoids any type of digital signal processing. Figure 2 details the nonlinear dynamical controller built around the identity $IQ' - QI' = rr' \sin(\theta - \theta')$, where I and Q are Cartesian components of baseband signals, r and θ are the corresponding polar coordinates, and primed coordinates denote symbols derived from the demodulated power amplifier output. Using the notation $\Delta\theta = \theta - \theta'$,

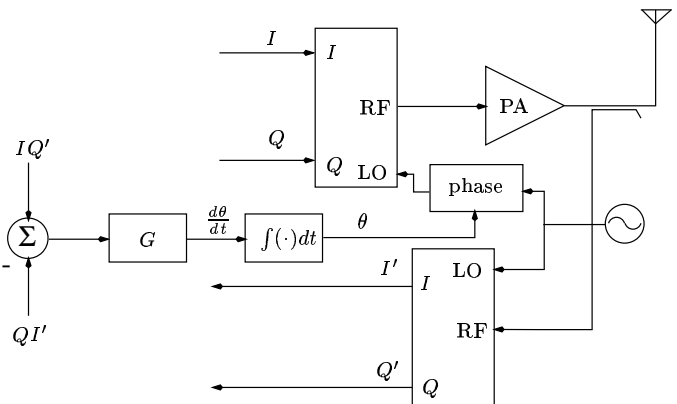


Fig. 2. System-level diagram of phase alignment system.

our circuit can be understood as mechanizing the equation

$$\frac{d\theta}{dt} = -\kappa[r(t)]^2 G \sin(\Delta\theta), \quad (1)$$

where κ is a constant of proportionality and gain G is associated with the integrator.

II. CONSEQUENCES OF PHASE MISALIGNMENT

The demodulated symbol S' is rotated relative to S by an amount equal to the local oscillator phase misalignment ϕ . To see this, we write the down-converted Cartesian components:

$$\begin{aligned} I' &= (I \sin \omega t + Q \cos \omega t) \sin(\omega t + \phi); \\ Q' &= (I \sin \omega t + Q \cos \omega t) \cos(\omega t + \phi); \end{aligned}$$

where ω is the carrier frequency. Using trigonometric identities and assuming frequency components at 2ω have been filtered out, we arrive at S' :

$$\begin{aligned} I' &= \frac{1}{2}(I \cos \phi + Q \sin \phi); \\ Q' &= \frac{1}{2}(-I \sin \phi + Q \cos \phi). \end{aligned}$$

Ideally, a Cartesian feedback loop functions as two identical, independent feedback systems. The reality of misalignment forces us to examine the dynamic behavior of two coupled loops. One method of analysis is to consider error signals $e_I(s)$ and $e_Q(s)$ as shown in Figure 3. We

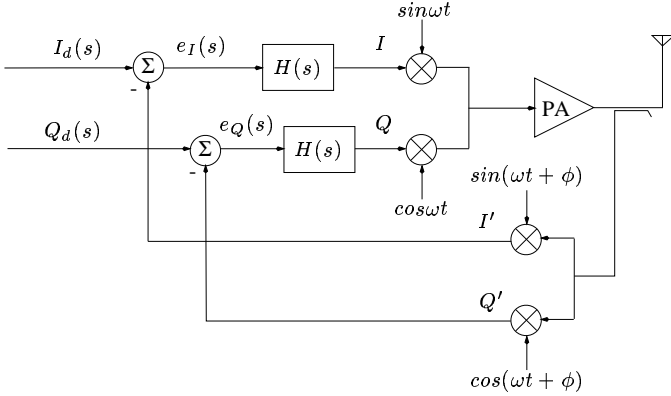


Fig. 3. Loop dynamics.

know that for a single feedback loop, the error signal can be written in the frequency domain as

$$e(s) = \frac{X(s)}{1 + L(s)}.$$

Here, $L(s)$ represents all dynamics in the loop and $X(s)$ is the input. For frequencies of interest, the hope is that $|L(s)|$ is very large.

In our case, let the phase misalignment be ϕ . Furthermore, we set $Q_d = 0$ without loss of generality¹. The error expressions, as a function of the single input $I_d(s)$, are now written:

$$\begin{aligned} e_I(s) &= I_d(s) - L(s)e_I(s) \cos \phi - L(s)e_Q(s) \sin \phi; \\ e_Q(s) &= L(s)e_I(s) \sin \phi - e_Q(s)L(s) \cos \phi. \end{aligned}$$

where $L(s)$ includes the dynamics of the loop compensation scheme ($H(s)$) and the (linearized) dynamics introduced by the modulator, power amplifier, and demodulator. From here, it is straightforward to show that

$$e_I(s) = \frac{X(s)}{1 + L(s) \cos \phi + \frac{[L(s) \sin \phi]^2}{1 + L(s) \cos \phi}}.$$

This reduction of the system to a single-input problem now yields considerable insight. We identify an effective loop transmission, $L_{\text{eff}}(s, \phi)$, as follows:

¹We do not lose generality as long as we stay with linearized analysis.

$$L_{\text{eff}}(s, \phi) = L(s) \cos \phi + \frac{[L(s) \sin \phi]^2}{1 + L(s) \cos \phi}. \quad (2)$$

For perfect alignment, $\phi = 0$ and L_{eff} is simply $L(s)$. The worst alignment is $\phi = \frac{\pi}{2}$, for which $L_{\text{eff}} = [L(s)]^2$: the loop dynamics are a cascade of the dynamics in the uncoupled case. Unless designed with this possibility in mind, most choices of $H(s)$ will yield unstable behavior in this second case. Equation 2 shows that traditional measures of stability will degrade continuously as ϕ sweeps from 0 to $\frac{\pi}{2}$. This was demonstrated experimentally by Briffa and Faulkner [3].

III. ALIGNMENT SYSTEM: STABILITY CONCERNS

Our control solution for the phase alignment problem is the simplest of nonlinear dynamical feedback systems. It can be seen from equation 1 to have two equilibrium points: the first, for which the symbols are aligned, is *stable*; the second, for which the symbols are misaligned by π radians, is *unstable*. For the ideal system represented by equation 1, this is the extent of a rigorous stability analysis.

The real-world situation can be complicated by dynamics associated with the phase shifter (and, possibly, the subtractor). If we consider a modulation scheme in which the magnitude of transmitted symbols is held constant², $r(t)$ in equation 1 loses its time dependence. Linearizing for small phase misalignments, and including the dynamics of the phase shifter as $P(s)$, we can represent the system as shown in figure 4. Drawing the system this way re-

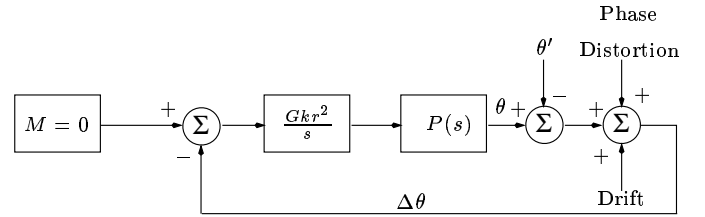


Fig. 4. Linearized phase regulation system; 'M' is desired misalignment.

quires some manipulation. The output of the phase shifter is not really θ , but rather an additive *part* of θ that gets combined with the polar angle of the symbol being transmitted. However, in the absence of phase distortion and drift, the symbol-by-symbol changes of the polar angle θ are tracked by identical changes in θ' . These symbol-rate changes are thus invisible to an alignment system, and it is appropriate to label the output of $P(s)$ as θ . We can then include the effects of phase distortion and phase alignment drift as the additive disturbances shown in figure 4.

One can ensure stability by choosing G such that, for the largest symbol magnitude, loop crossover occurs before non-dominant poles become an issue. Fortunately, the drift

²Highly improbable when using Cartesian feedback, of course. Temporarily making this assumption, however, yields insight that is broadly relevant.

disturbance will normally occur on the time scales associated with temperature drift and aging [5]. Suppression of the phase distortion is the domain of the Cartesian feedback itself. It follows that for many systems, little of the design effort need be focused on fast phase alignment.

IV. IMPLEMENTATION

Our prototype can be divided into two basic functional blocks: the phase shifter and the controller itself. In this section we describe each in turn, and follow with a discussion of the impact of circuit nonidealities on the system's performance.

A. Phase Shifter

The phase shifter was implemented using a quadrature modulator and an analog control loop, as shown in figure 5. This control loop forces the sum of the squares of the mod-

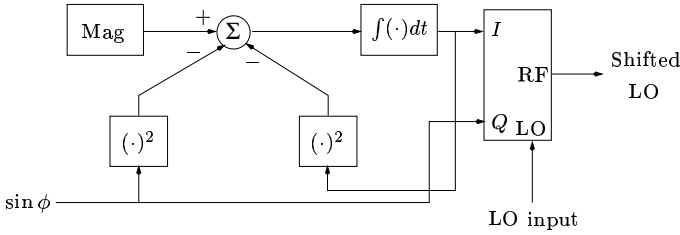


Fig. 5. Phase shifter.

ulator inputs to equal a constant ('Mag'), thereby ensuring a constant amplitude for the shifted LO. This actually introduces a small change in the math: we write the shifted LO as

$$I_{LO} \sin \omega t + Q_{LO} \cos \omega t.$$

To within a multiplicative constant, this is equal to

$$\cos \phi \sin \omega t + \sin \phi \cos \omega t.$$

For this prototype, then, the analog input is proportional to the *sine* of the phase shift. A functional block labeled 'arcsin(.)' effectively exists between the integrator output and phase shifter input in figure 2.

The complete phase shifter, together with the rest of the controller, is shown in figure 6. Because of the squaring functional blocks, there are in general two values of I_{LO} that would satisfy the control loop. The sign of the incremental gain around the loop is positive for one solution and negative for the other. The comparator in figure 6 ensures stability by switching the sign of the loop gain based on the current value of I_{LO} .

The switches on all of the integrators were purely for testing purposes and were manually operated. These familiar "3-mode integrators" allowed the outputs of the integrators to be held at their last value, to be manually adjusted with potentiometers, or to operate normally as integrators.

B. Controller

The controller represents a straightforward mapping from figure 2 to op-amp building blocks. As will be discussed in subsection IV-C, it was necessary to trim the output offsets of the AD835 multipliers (from Analog Devices). This trimming was crudely accomplished via a potentiometer connected to the summing input of one of the multipliers.

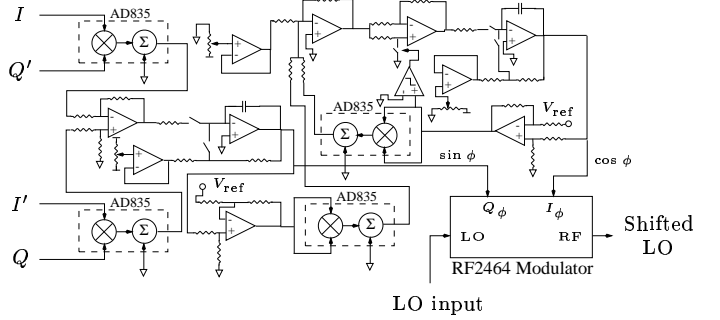


Fig. 6. Nonlinear dynamical controller and phase shifter implementation.

C. Impact of circuit nonidealities

The ability to accurately regulate the phase alignment depends on the ability to accurately calculate $IQ' - QI'$. Offsets associated with the output buffers of the multipliers and the input of the integrator are particularly troublesome. Consider an input-referred offset of δ for the controller integrator, and its effect on the final alignment. We write

$$\frac{d\theta}{dt} = G[-\kappa[r(t)]^2 \sin(\Delta\theta) + \delta] = 0.$$

For our prototype κ was approximately $1.3V^{-1}$. For a symbol magnitude of 50mV, we can solve for the offset that results in a 5-degree final misalignment:

$$\delta = (1.3V^{-1})(50mV)^2 \sin\left(\frac{2\pi(5)}{360}\right) = 283\mu V.$$

This example illustrates one of the major challenges that the analog multipliers introduce: offsets become increasingly intrusive as symbol magnitudes decrease. A 5-degree misalignment for a symbol magnitude of a volt leads to a δ of 113mV; for a symbol magnitude of 1mV, $\delta = .113\mu V$.

Mitigating this effect is the fact the controller slows for smaller signals: until offsets dominate, $|\frac{d\theta}{dt}|$ scales linearly with $[r(t)]^2$. These numbers nevertheless suggest that, in some implementations, it may be necessary to prescale the inputs of the multipliers according to the known symbol magnitudes.

In our prototype, the bandwidth of the op-amp subtractor proved to be a limitation as well. This needn't be true in a monolithic implementation, however: accurate subtraction in the current domain is trivially implemented, and many multiplier topologies provide output in the form of currents.

V. RESULTS

The prototype shown in figure 6 was built and tested in a 250 MHz RF system. Figure 7 shows the test setup. An

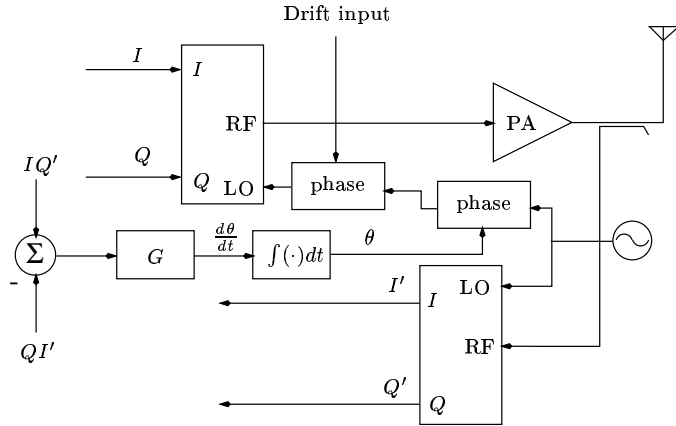


Fig. 7. Test setup.

additional phase shifter was inserted in the control path and was manually controlled. By varying this phase shift, we simulated drift normally due to temperature and aging. Figure 8 shows the outcome of this experiment. The I channel was driven with a 50mV sinusoid, and the Q channel was grounded. It can be seen that our prototype auto-

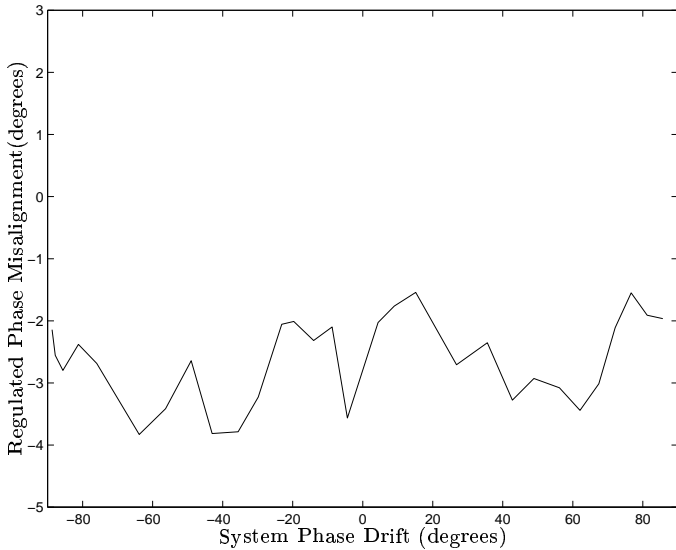


Fig. 8. Measured phase alignment vs. system drift

matically and continuously compensates for misalignments as large as ± 88 degrees. Alignment to within 3.8 degrees is maintained over this entire range of disturbances.

Figure 9 shows system performance as the frequency of the input sinusoid is varied. It is seen that performance deteriorates rapidly above 2 MHz. This was due to the op-amp used to build the subtractor (National Semiconductor's LMC6484), which has a gain-bandwidth product of 1.5MHz.

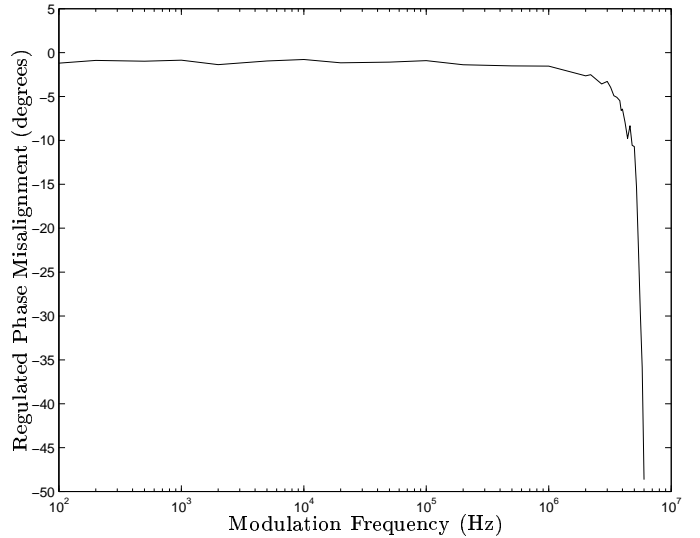


Fig. 9. Phase alignment vs. Baseband Frequency

The following table³ compares the prototype with other examples from the literature.

Work	Accuracy	Baseband Bandwidth	Carrier (GHz)
This work	3.8 degrees	2 MHz	.25
[2]	10 degrees	21 kbaud	.90
[4]	not reported	25 kHz	.22
[1]	15 degrees	500 kbaud	.90

TABLE I

COMPARISON WITH EXAMPLES FROM THE LITERATURE.

VI. CONCLUSIONS

The inability to continuously regulate phase alignment has been a major barrier to the widespread use of Cartesian feedback as a linearization technique [5]. We believe this work has the potential to lower that barrier considerably, making it easier to build a Cartesian feedback system that can operate maintenance-free in a hostile environment.

REFERENCES

- [1] Mats Johansson. Linearization of rf power amplifiers using cartesian feedback. Technical report, Lund University.
- [2] Y. Ohishi, M. Minowa, E. Fukuda, and T. Takano. Cartesian feedback amplifier with soft landing. In *3rd IEEE International Symposium on Personal, Indoor, and Wireless Communications*, pages 402–406, 1992.
- [3] M. Briffa and M. Faulkner. Gain and phase margins of cartesian feedback rf amplifier linearisation. *Journal of Electrical and Electronics Engineering, Australia*, 14:283–289, December 1994.
- [4] Majid Boloorian and Joseph McGeehan. The frequency-hopped cartesian feedback linear transmitter. *IEEE Trans. on Vehicular Technology*, 45:688–706, November 1996.
- [5] B. Razavi. *RF Microelectronics*. Prentice-Hall, Inc., Upper Saddle River, NJ, 1998.

³Accuracy value for Ohishi et al. is inferred.